ACS Catalysis

Letter

pubs.acs.org/acscatalysis

Diffusion-Driven Selectivity in Oxidation of CO in the Presence of Propylene Using Zeolite Nano Shell as Membrane

Shiwen Li, Cindy Aquino, Laurent Gueudré, Alain Tuel, Yves Schuurman, and David Farrusseng*

IRCELYON, UMR 5256 CNRS- Université Lyon-1, 2 Avenue Albert Einstein, F-69626 Villeurbanne, France

Supporting Information

ABSTRACT: The selective oxidation of CO over C_3H_6 is achieved in yolk-shell Pt@Silicalite-1 catalysts in which Pt nanoparticles are encapsulated in hollow silicalite-1 single crystals. The thin shell operates as a permselective membrane which limits Pt surface poisoning by C_3H_6. From adsorption measurements, we conclude that the catalytic selectivity arises from the fastest diffusion of CO over C_3H_6 through the silicalite-1 membrane.

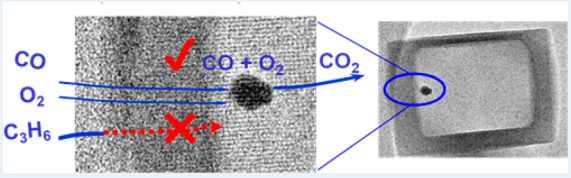

KEYWORDS: *heterogeneous catalysis, Pt nanoparticle, hollow zeolite, selective CO oxidation, poison resistance, diffusion*

The design of acid catalysts by shape selectivity is well established. It deals with the molecular sieving of different substrates/products or preventing the formation of intermediates bulkier than the cavity of zeolite. Such type of selective catalysts are used at industrial scales for major chemical and energy processes such as disproportionation of toluene,[1] alkylation,[2] and MTO.[3] On the other hand, selective oxidation/reduction on metal catalysts is achieved by designing the metal surface with appropriate adsorption features so that the adsorption of the target substrate can be selectively converted.[4−7] Selectivity is addressed by playing on surface sensitivity[8] and alloying effects.[4] Carbon monoxide and alkenes strongly compete for adsorption on noble metal surfaces.[9] The presence of a very small concentration of CO decreases the activity of the hydrogenation of ethylene by several orders of magnitude.[10] Conversely, the process of selective CO oxidation in the presence of alkenes for purification purposes is also a scientific and technical challenge.[9,11,12]

Lately, the concept of controlling the selectivity of metal catalysts by a shell of zeolite membrane was reported. Collier et al. demonstrated the CO selective oxidation in the presence of butane achieved by a zeolite-coated metal/SiO_2 catalyst.[13,14] Kapteijn et al. described a H-ZSM-5-coated Co/SiO_2 catalyst capable of producing a certain range of hydrocarbons in Fischer−Tropsch synthesis.[15−17] Nishiyama et al. showed transport-driven selective hydrogenation on a mixture of linear and branched C_6 alkenes on Pt/TiO_2 beads coated with silicalite-1 polycrystalline layer.[18,19] In all previous studies, a macroscopic layer is coated on metal/SiO_2 grains, and the activity is given by the metal particles underneath the membrane. However, the thickness of the zeolite shell is usually from 200 nm up to several microns,[14,18] which eventually limits the overall reaction rates due to diffusion transport limitations.[18]

The so-called "yolk−shell catalyst" design is an attractive solution which can overcome diffusion limitation. Yolk−shell catalysts are specific materials in which the yolk is a catalyst particle and the shell is a very thin porous layer, generally an inorganic oxide (ZrO_2, TiO_2, and SiO_2) or carbon.[20−24] Recently, PtCo bimetallic nanoparticles encapsulated in carbon hollow spheres were reported for outstanding performances in the hydrogenolysis of HMF to DMF by the group of F. Schüth.[25] This catalyst demonstrated an enhancement in the production of molecular fuel from biomass over the metal catalysis. However, mesoporous shells are not appropriate to separate gas molecules such as light hydrocarbons and permanent gases(CO, CO_2,N_2, etc.) because of the mismatch between the size of membrane cavities (>2 nm) and the sieve of substrates (kinetic diameter <1 nm), thus preventing a sieving separation mechanism.

Recently, we have reported the synthesis of yolk−shell materials which consist of metal nanoparticles (Au, Pt) encapsulated in hollow crack-free silicalite-1 single crystals with a wall thickness of about 20 nm. This enables the preparation of isolated metal nanoparticles with size control from 1 to 10 nm and narrow distribution.[26] The concept of selective hydrogenation driven by molecular sieving property of the reactants using a zeolite shell has been illustrated on a Pt@ hollow silicalite-1.[27] We have shown that toluene (0.61 nm, kinetic diameter) is hydrogenated, whereas mesitylene (0.87 nm, kinetic diameter), which has a larger kinetic diameter than the pore size of siliclaite-1 (0.55 nm), is not.

Unfortunately, for light hydrocarbons and permanent gases, the size exclusion mechanism cannot operate because they can all penetrate into the microporous network. Nevertheless, we can assume that the differences in diffusion rates between two substrates in zeolite membrane shall result in a selective separation, that is, the permselective transport of one reactant through a zeolite layer could enhance catalytic selectivity.[28−30]

Received: September 7, 2014
Revised: October 29, 2014
Published: November 1, 2014

   dx.doi.org/10.1021/cs501349b | ACS Catal. 2014, 4, 4299−4303

In this study, we have applied Pt nanoparticles encapsulated in thin hollow zeolite shells, hereafter called "Pt@S-1", as effective CO selective oxidation catalysts in the presence of propylene acting as a poison. We demonstrate that the zeolite shell limits transport of propylene to the metal particles while CO is converted by Pt nanoparticles. Two reference catalysts were prepared and tested in order to support our hypothesis.

A detailed recipe of Pt@S-1 "yolk shell" catalyst can be found in previous publications and in the Supporting Information (SI).[27,31] In brief, Pt@S-1 is obtained by treating Pt impregnated silicalite-1 in TPAOH solution at 170 °C. Each hollow shell is approximately 200 nm × 150 nm × 140 nm in size and contains one Pt particle (Figure 1) (less than 5%

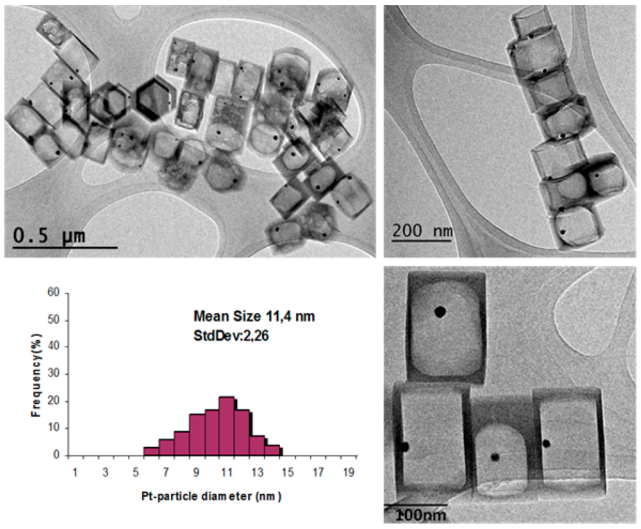

Figure 1. TEM images of Pt@S-1 and size distribution of Pt particles.

hollow zeolites contain more than 1 particle). The HRTEM picture and X-ray diffraction clearly show the single crystal nature of the 20 nm thick walls without apparent defects such as twinning planes, grain boundary zones, or pinholes (see Figure S1). The hollow zeolites are mechanically robust as they cannot be broken upon manual grinding with a mortar and they do not collapse when pressing up to 5 tons. Nitrogen physisorption measurements (at 77 K) are similar to those previously reported for Pt-free hollow silicalite-1 (see Figure S2).[31]

In contrast to materials made of a polycrystalline zeolite shell, the presence of a hysteretic loop with a forced closure at $p/p_0 \approx 0.45$ indicates that the walls of the hollow zeolite do not contain pores larger than 4 nm.[32,33] The mean size of Pt particles of Pt@S-1 has been calculated from size distribution population of 400 particles measured by TEM (Figure 1).[34] The particle size distribution is relatively narrow. More than 50% of particles are between 10 to 12 nm in diameter.

Catalytic data are compared with (0.90 wt %) Pt-supported silicalite-1 (Pt/S-1). It is produced by using the same starting materials as Pt@S-1 but without the TPAOH post-treatment step, which is responsible for desilication (details in SI). Pt/S-1 is characterized by a significant portion of the Pt particles located at the external surfaces (Figure S3), whereas others are embedded in the zeolite crystals. A commercial Pt/SiO_2 supported catalyst obtained from Sigma-Aldrich (0.71 wt % Pt, Figure S4) is used as a second reference sample. The three catalysts are quite similar in terms of Pt loadings and mean Pt particle sizes; 11.4, 8.9, and 7.5 nm for Pt@S-1, Pt/S-1, and Pt/SiO_2, respectively (Table S1). The catalysts differ on the location of the Pt nanoparticles. In Pt@S-1, the Pt particles are encapsulated inside a silicalite-1 box, whereas for the two reference catalysts, the particles are directly accessible to the gas phase. The mechanism of formation of the Pt nanoparticles at the external surface of silicalite-1 crystal in Pt/S-1 goes beyond the scope of this study. Nevertheless, we can assume that during the heat treatment the Pt atoms and/or cluster may diffuse through the zeolite channels to the surface where they can grow.

CO oxidation with or without propylene was carried out in a fixed bed reactor by rising the temperature at a constant rate of 1 °C/min. The compositions (vol %) of the stream were 2% CO, 2% C_3H_6 (when present), 2% O_2 and balance of N_2. As a consequence, O_2 is in excess for the selective oxidation of CO, whereas it is a default for a total combustion of C_3H_6. Molar fractions of reactants and products were measured by a fast-gas chromatograph allowing an analysis every 4 min. The conversions of CO and C_3H_6 (if present) are plotted as a function of the catalyst bed temperature for Pt@S-1 and the reference Pt/S-1 (Pt/SiO_2 in SI, Figure S5) catalysts (Figure 2).

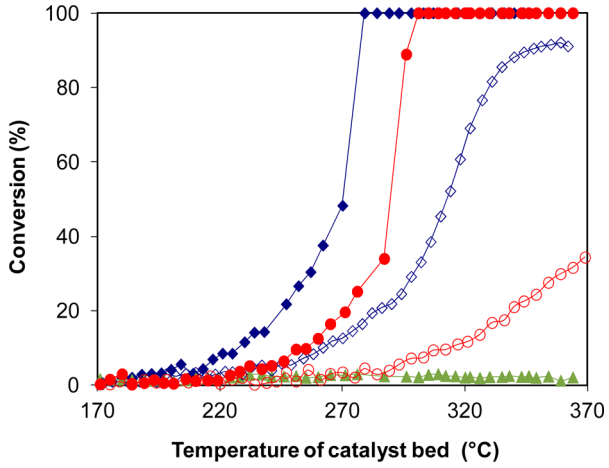

Figure 2. CO conversion in the absence (full symbols) and in the presence (open symbols) of propylene over Pt@S-1(blue ◆, blue ◇), Pt/S1(red ●, red ○), and metal-free hollow silicalite-1(green ▲).

In the absence of propylene, Pt-free hollow silicalite-1 shows a negligible activity, and the CO conversion does not exceed 3%. All Pt-containing catalysts fully convert CO with light-off temperatures between 270 and 310 °C (see Table S2), in good agreement with data from the literature.[35] The origin of the small variation of the light-off temperature for the three samples may be due to the slightly different Pt loading used in the testing (i.e., 0.44, 0.45, and 0.35 mg for Pt@S-1, Pt/S-1, and Pt/SiO_2 (see Table S2), which was also confirmed by CO oxidation catalyzed by different amounts of Pt@S-1 catalyst (see Figure S6 and Table S3).

The introduction of 2% C_3H_6 significantly shifts the light-off temperature of all three catalysts. More importantly, it strongly reduces conversion for the reference catalysts Pt/S-1 and Pt/SiO_2, both exhibiting very similar results (see Figure S5). For these two reference catalysts, the maximum CO conversion reaches only 35−40% at 370 °C with light-off temperatures of ca. 340 °C. As already described by Voltz,[9] propylene partially prevents the adsorption of CO on Pt particles and therefore acts as a surface reversible poison. By contrast to the above

dx.doi.org/10.1021/cs501349b | ACS Catal. 2014, 4, 4299−4303

benchmark catalysts, Pt@S-1 remains highly active in the presence of propylene. Maximum CO conversion reaches 92% at 360 °C, which is more than twice the reference catalysts. At 280 °C, the TOFs (turnover frequencies) over Pt@S-1 are 4 and 8 times larger than over Pt/S-1 in CO oxidation in the absence and presence of propylene, respectively (see Table S2). In addition, the three catalysts' propylene conversions at 350 °C are 2.4%, 4%, and 1.3% over Pt@S-1, Pt/S-1, and Pt/SiO_2 catalysts, respectively (see Figure S5). Pt@S-1 showed the highest CO conversion with limited propylene oxidation. For Pt/SiO_2, all Pt particles are directly accessible to the gas phase and therefore are subject to propylene poisoning. The same applies for Pt/S-1, where most of the Pt particles are located at the external surfaces of the zeolite crystals. It is therefore not surprising that Pt/SiO_2 and Pt/S-1 reference catalysts perform similarly. Moreover, we do not observe any change in the color of the catalyst before and after reaction. The carbon balance for each reaction is generally above 98%, which suggests that the amount of coke formed is negligible.

Obviously, the selective permeability of zeolite shells limits the poisoning effect of propylene while maintaining a high accessibility to carbon monoxide. The transport properties of silicalite-1 and permeation properties of silicalite-1 membranes are well-known and support our hypothesis.

The kinetic diameters of CO (0.376 nm) and C_3H_6 (0.45 nm) are smaller than the pore size of silicalite-1 (0.51 nm × 0.55 nm). Hence, a steric exclusion mechanism cannot be proposed for supporting the catalytic results. For a silicalite-1 membrane, it is acknowledged that the separation mechanism of a mixture of substrates depends first on coverage concentrations of the different species.[36,37] At high coverage, the most strongly adsorbed substrate prevents other substrates from adsorption and thus diffusion. However, at these reaction temperatures (T > 200 °C), we estimate from adsorption isotherm data that the fractional coverage of CO and propylene are lower than 1% (see Figures 3, 4, and S4 and Table1).

Thus, competitive adsorption can be ruled out for the limitation of the transport of propylene. The second mechanism of membrane permselectivity is driven by differences in diffusion rates which are mainly governed by the size of the substrate.[36,38] The effective mass transfer coefficient (Kap) of CO and propylene were measured at low coverage on

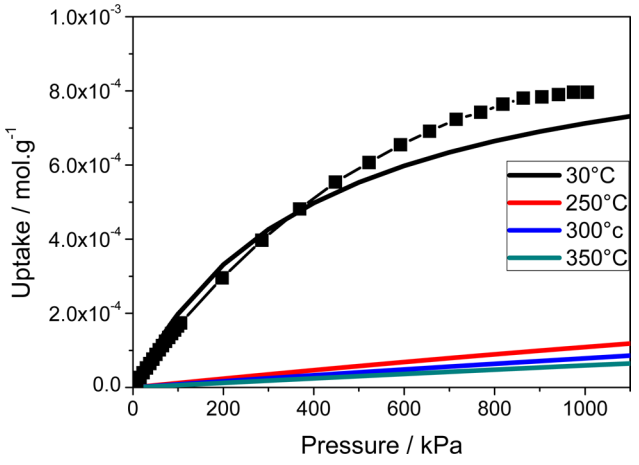

Figure 3. CO adsorption isotherms. Experimental data at 30 °C (full line), fitted data at 30 °C (black square), simulated data at 250, 300, 350 °C.

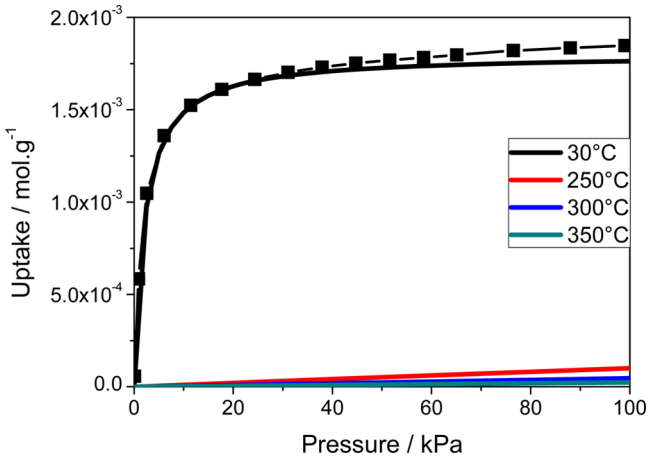

Figure 4. C_3H_6 adsorption isotherms. Experimental data at 30 °C (full line), fitted data at 30 °C(black square), simulated data at 250, 300, 350 °C.

Table 1. Coverage Estimations at Room Temperature and Reaction Conditions for Partial Pressures of 2 kPa

temp	30 °C	250 °C	300 °C	350 °C
coverage	%	%	%	%
CO	<1	<1	<1	<1
C_3H_6	90.4	1.2	<1	<1

hollow silicalite-1 in a volumetric measurement system by applying the Linear Driving Force Model (LDF) (Figure 5).[39] We calculate that at room temperature C_3H_6 diffuses more than 200 times slower than CO, which could explain the permselective mechanism of the zeolite shell and thus the poisoning CO resistance of the Pt@S-1 catalyst. Because C_3H_6 can diffuse through the membrane, C_3H_6 can still poison the Pt surface as the concentration of C_3H_6 builds up with time in the hollow zeolite, whereas the CO is depleted by oxidation. The estimation evolution of partial pressure of C_3H_6 and other components at reaction temperature with time would require the modeling of the catalytic and all transport phenomena including the retrodiffusion of CO_2, which is beyond the scope of this study.

We report here an original synthesis pathway for Pt nanoparticles encapsulated in a defect-free, hollow single crystal zeolite with shells around 20 nm thick. In contrast to a classical Pt-impregnated silicalite-1, the hollow zeolite shell prevents Pt particles to grow at the external surface of the crystal. This type of yolk−shell catalyst, which is characterized by large hollow cavities, is minimally appropriate for practical application as the low metal density will result in very large catalyst volume. We showed earlier for gold@silicalite-1 that an increase of 90 times particles concentration can be achieved by starting with larger zeolite crystals.[26] We will report shortly a detailed study of the synthesis process for loading larger number of nanoparticles. We demonstrate for the first time that a single crystal zeolite shell can also act as a permselective membrane which prevents the encapsulated metal particles from poisoning. In the case of CO oxidation in the presence of the reversible poison propylene, the separation mechanism is driven by the difference in the diffusion rates between CO and propylene, the latter being more than 200 times slower at room temperature.

dx.doi.org/10.1021/cs501349b | ACS Catal. 2014, 4, 4299−4303

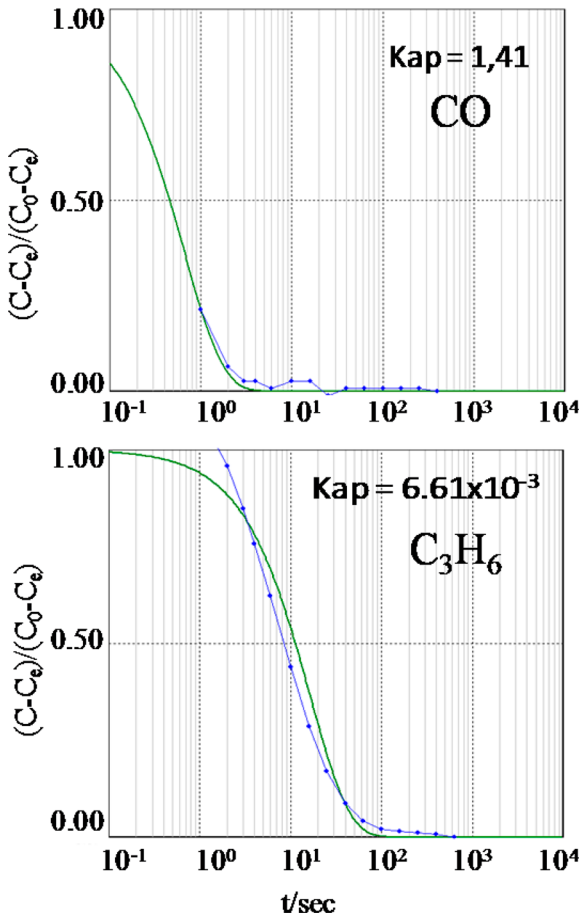

Figure 5. Relaxation pressure in the adsorption of CO (up) and C_3H_6 (down) at 30 °C and corresponding at coverage of 10% (blue squares). LDF model fit (green line).

■ ASSOCIATED CONTENT

Supporting Information

The following file is available free of charge on the ACS Publications website at DOI: 10.1021/cs501349b.

Material preparation, elementary analysis, single adsorption measurements, and breakthrough experiments (PDF).

■ AUTHOR INFORMATION

Corresponding Author

*E-mail: david.farrusseng@ircelyon.univ-lyon1.fr.

Notes

The authors declare no competing financial interest.

■ ACKNOWLEDGMENTS

The authors thank the scientific services of IRCELYON. This study has been supported by the European Union Seventh Framework Programme FP7-NMP-2010, under Grant Agreement No. 263007 (acronym CARENA).

■ REFERENCES

(1) Xiong, Y.; Rodewald, P. G.; Chang, C. D. *J. Am. Chem. Soc.* **1995**, *117*, 9427−9431.
(2) Chen, N. Y.; Garwood, W. E. *Catal. Rev.: Sci. Eng.* **1986**, *28*, 185−264.
(3) Olsbye, U.; Svelle, S.; Bjørgen, M.; Beato, P.; Janssens, T. V. W.; Joensen, F.; Bordiga, S.; Lillerud, K. P. *Angew. Chem., Int. Ed.* **2012**, *51*, 5810−5831.
(4) Studt, F.; Abild-Pedersen, F.; Bligaard, T.; Sørensen, R. Z.; Christensen, C. H.; Nørskov, J. K. *Science* **2008**, *320*, 1320−1322.
(5) Bond , G. *Catalysis by Metals* ; Academic Press : New York , 1962 .
(6) Toulhoat, H.; Raybaud, P. *J. Catal.* **2003**, *216*, 63−72.
(7) Corvaisier, F.; Schuurman, Y.; Fecant, A.; Thomazeau, C.; Raybaud, P.; Toulhoat, H.; Farrusseng, D. *J. Catal.* **2013**, *307*, 352−361.
(8) Sachtler, W. M. H.; Van Santen, R. A. *Adv. Catal.* **1977**, *26*, 69−119 DOI: 10.1016/S0360-0564(08)60070-X.
(9) Voltz, S. E.; Morgan, C. R.; Liederman, D.; Jacob, S. M. *Ind. Eng. Chem. Prod. Res. Dev.* **1973**, *12*, 294−301.
(10) Rioux, R. M.; Komor, R.; Song, H.; Hoefelmeyer, J. D.; Grass, M.; Niesz, K.; Yang, P.; Somorjai, G. A. *J. Catal.* **2008**, *254*, 1−11.
(11) Patience, G. S.; Benamer, A.; Chiron, F. X.; Shekari, A.; Dubois, J. L. *Chem. Eng. Process. Process Intensif.* **2013**, *70*, 162−168.
(12) Koermer , G. S. ; Hratko , L. ; U.S. Patent No. 6,548,446/B1, April 15, 2003 .
(13) Collier, P.; Golunski, S.; Malde, C.; Breen, J.; Burch, R. *J. Am. Chem. Soc.* **2003**, *125*, 12414−12415.
(14) Devi, R. N.; Meunier, F. C.; Le Goaziou, T.; Hardacre, C.; Collier, P. J.; Golunski, S. E.; Gladden, L. F.; Mantle, M. D. *J. Phys. Chem. C* **2008**, *112*, 10968−10975.
(15) He, J.; Yoneyama, Y.; Xu, B.; Nishiyama, N.; Tsubaki, N. *Langmuir* **2005**, *21*, 1699−1702.
(16) Sartipi, S.; van Dijk, J. E.; Gascon, J.; Kapteijn, F. *Appl. Catal., A* **2013**, *456*, 11−22.
(17) Sartipi, S.; Makkee, M.; Kapteijn, F.; Gascon, J. *Catal. Sci. Technol.* **2014**, *4*, 893−907.
(18) Miyamoto, M.; Kamei, T.; Nishiyama, N.; Egashira, Y.; Ueyama, K. *Adv. Mater.* **2005**, *17*, 1985−1988.
(19) Nishiyama, N.; Ichioka, K.; Park, D.-H.; Egashira, Y.; Ueyama, K.; Gora, L.; Zhu, W.; Kapteijn, F.; Moulijn, J. A. *Ind. Eng. Chem. Res.* **2004**, *43*, 1211−1215.
(20) Arnal, P. M.; Comotti, M.; Schüth, F. *Angew. Chem., Int. Ed.* **2006**, *45*, 8224−8227.
(21) Lee, I.; Joo, J. B.; Yin, Y.; Zaera, F. *Angew. Chem., Int. Ed.* **2011**, *50*, 10208−10211.
(22) Joo, S. H.; Park, J. Y.; Tsung, C.-K.; Yamada, Y.; Yang, P.; Somorjai, G. A. *Nat. Mater.* **2009**, *8*, 126−131.
(23) Galeano, C.; Guettel, R.; Paul, M.; Arnal, P.; Lu, A.-H.; Schüth, F. *Chem.—Eur. J.* **2011**, *17*, 8434−8439.
(24) Ikeda, S.; Ishino, S.; Harada, T.; Okamoto, N.; Sakata, T.; Mori, H.; Kuwabata, S.; Torimoto, T.; Matsumura, M. *Angew. Chem., Int. Ed.* **2006**, *45*, 7063−7066.
(25) Wang, G.-H.; Hilgert, J.; Richter, F. H.; Wang, F.; Bongard, H.-J.; Spliethoff, B.; Weidenthaler, C.; Schüth, F. *Nat. Mater.* **2014**, *13*, 293−300.
(26) Li, S.; Burel, L.; Aquino, C.; Tuel, A.; Morfin, F.; Rousset, J.-L.; Farrusseng, D. *Chem. Commun.* **2013**, *49*, 8507−8509.
(27) Li, S.; Boucheron, T.; Tuel, A.; Farrusseng, D.; Meunier, F. *Chem. Commun.* **2014**, *50*, 1824−1826.
(28) van der Puil, N.; Creyghton, E. J.; Rodenburg, E. C.; Sie, T. S.; van Bekkum, H.; Jansen, J. C. *J. Chem. Soc., Faraday Trans.* **1996**, *92*, 4609−4615.
(29) van der Puil , N. ; Janto-Saputro , I. B. ; van Bekkum , H. ; Jansen , J. C. In *Stud. Surf. Sci. Catal.* ; Hakze Chon , S.-K. I. , Young Sun , U. , Eds.; Elsevier : 1997 , *105* , 1341 − 1348 .
(30) van der Puil, N.; Dautzenberg, F. M.; van Bekkum, H.; Jansen, J. C. *Microporous Mesoporous Mater.* **1999**, *27*, 95−106.
(31) Wang, Y.; Tuel, A. *Microporous Mesoporous Mater.* **2008**, *113*, 286−295.
(32) Groen, J. C.; Perez-Ramirez, J. *Appl. Catal., A* **2004**, *268*, 121−125.
(33) Groen, J. C.; Peffer, L. A. A.; Pérez-Ramírez, J. *Microporous Mesoporous Mater.* **2003**, *60*, 1−17.

(34) Quinet, E.; Morfin, F.; Diehl, F.; Avenier, P.; Caps, V.; Rousset, J.-L. *Appl. Catal., B* **2008**, *80*, 195−201.
(35) Alayon, E. M. C.; Singh, J.; Nachtegaal, M.; Harfouche, M.; Van Bokhoven, J. A. *J. Catal.* **2009**, *263*, 228−238.
(36) Savitz, S.; Myers, A. L.; Gorte, R. J. *J. Phys. Chem. B* **1999**, *103*, 3687−3690.
(37) Hampson, J. A.; Rees, L. V. C. *J. Chem. Soc., Faraday Trans.* **1993**, *89*, 3169−3176.
(38) van de Graaf, J. M.; Kapteijn, F.; Moulijn, J. A. *AIChE J.* **1999**, *45*, 497−511.
(39) Sircar, S.; Hufton, J. *Adsorption* **2000**, *6*, 137−147.